Published OnlineFirst October 25, 2017; DOI: 10.1158/2326-6066.CIR-17-0341

Research Article

Cancer Immunology Research

Interleukin-12 from CD103$^+$ Batf3-Dependent Dendritic Cells Required for NK-Cell Suppression of Metastasis

Deepak Mittal[1], Dipti Vijayan[1], Eva M. Putz[1], Amelia R. Aguilera[1], Kate A. Markey[2,3], Jasmin Straube[4], Stephen Kazakoff[4], Stephen L. Nutt[5], Kazuyoshi Takeda[6], Geoffrey R. Hill[2,3], Nicola Waddell[4], and Mark J. Smyth[1]

Abstract

Several host factors may affect the spread of cancer to distant organs; however, the intrinsic role of dendritic cells (DC) in controlling metastasis is poorly described. Here, we show in several tumor models that although the growth of primary tumors in Batf3-deficient mice, which lack cross-presenting DCs, was not different from primary tumors in wild-type (WT) control mice, Batf3-deficient mice had increased experimental and spontaneous metastasis and poorer survival. The increased metastasis was independent of CD4$^+$ and CD8$^+$ T lymphocytes, but required NK cells and IFNγ. Chimeric mice in which Batf3-dependent DCs uniformly lacked the capacity to produce IL12 had metastatic burdens similar to the Batf3-deficient mice, suggesting that Batf3$^+$ DCs were the only cell type whose IL12 production was critical for controlling metastasis. We found that IL12-YFP reporter mice, whose lungs were injected with B16F10 melanoma, had increased numbers of IL12-expressing CD103$^+$ DCs with enhanced CD86 expression. Bone-marrow–derived DCs from WT, but not Batf3-deficient, mice activated NK cells to produce IFNγ in an IL12-dependent manner and therapeutic injection of recombinant mouse IL12 decreased metastasis in both WT and Batf3-deficient mice. Analysis of TCGA datasets revealed an association between high expression of *BATF3* and *IRF8* and improved survival of breast cancer patients; *BATF3* expression also significantly correlated with NK-cell receptor genes, *IL12*, and *IFNG*. Collectively, our findings show that IL12 from CD103$^+$ DCs is critical for NK cell–mediated control of tumor metastasis. *Cancer Immunol Res; 5(12); 1098–108. ©2017 AACR.*

Introduction

Cancer immunotherapy with immune checkpoint blockade and adoptive T-cell therapies has established the ability of a remobilized immune system to control tumor growth and metastasis and to improve the survival of cancer patients. Much of the success with immune checkpoint blockade and other immunomodulatory strategies has highlighted the critical role that efficient cross-presentation by dendritic cells (DCs) might play with respect to effector T-cell control of tumors (1–4). Yet the role of the DC in the control of metastasis is poorly characterized.

Conventional DCs (cDC) can be divided into two major groups. cDC1 consist of CD8α$^+$ tissue-resident or CD103$^+$ migratory DCs that are specialized for antigen cross-presentation. cDC2, or CD11b$^+$ DCs, directly present antigens via MHC class II. Cross-presenting DCs are of special interest because of their ability to phagocytose cellular proteins, directing them to the MHC class I antigen presentation pathway that will activate CD8$^+$ cytotoxic T cells (5, 6). Mice deficient in Batf3, Irf8, Id2, and Nfil3 have defects in the generation of CD8α$^+$ and CD103$^+$ DCs, suggesting that their development requires these transcription factors. In particular, Batf3-deficient mice show impaired ability to cross-prime cytotoxic T lymphocytes (CTL) against tumor antigens in immunogenic fibrosarcomas and lack virus-specific CTL responses to West Nile infection (7). Batf3-dependent DCs display strong protective Th1 type immune responses against the parasitic infections of *Toxoplasma gondii* (8) and *Leishmania* (9, 10) that were dependent on IL12 secretion. Batf3 deficiency also increased resistance to helminth infections by augmenting Th2 type immunity, which was dependent on constitutive expression of IL12 by CD103$^+$ Batf3-dependent DCs, but was independent of Toll-like receptors or microbial signals (11). In contrast, the Batf3 deficiency was dispensable for antifungal immune responses (12).

Batf3 DCs are the major producers of IL12 and secretion of IL12 from these DCs is the one of the main mechanisms for controlling infection and cancer (3, 8–10, 13–15). Batf3 deficiency abrogated

[1]Immunology in Cancer and Infection Laboratory, QIMR Berghofer Medical Research Institute, Herston, Queensland, Australia. [2]Bone Marrow Transplantation Laboratory, QIMR Berghofer Medical Research Institute, Herston, Queensland, Australia. [3]Department of Haematology, Royal Brisbane Hospital, Herston, Queensland, Australia. [4]Medical Genomics Laboratory, QIMR Berghofer Medical Research Institute, Herston, Queensland, Australia. [5]Walter and Eliza Hall Institute of Medical Research and Department of Medical Biology, University of Melbourne, Parkville, Victoria, Australia. [6]Division of Cell Biology, Biomedical Research Center, Graduate School of Medicine, Juntendo University, Bunkyo-ku, Tokyo, Japan.

Note: Supplementary data for this article are available at Cancer Immunology Research Online (http://cancerimmunolres.aacrjournals.org/).

Corresponding Authors: Mark J. Smyth, QIMR Berghofer Medical Research Institute, 300 Herston Road, Herston 4006, Australia. Phone: 61-7-8345-3957; Fax: 61-7-3362-0111; E-mail: mark.smyth@qimrberghofer.edu.au; and Deepak Mittal, Immunology in Cancer and Infection Laboratory, QIMR Berghofer Medical Research Institute, Herston, Queensland 4006, Australia. Phone: 61-7-3845-3023; E-mail: deepak.mittal@qimrberghofer.edu.au

doi: 10.1158/2326-6066.CIR-17-0341

Published OnlineFirst October 25, 2017; DOI: 10.1158/2326-6066.CIR-17-0341

the antitumor efficacy of the combination of anti-CD137 and anti–PD-1 immunotherapies that was not rescued by IL12 administration (1). Although CD8α$^+$ Batf3-dependent DCs were indispensable for TRAIL-based immunotherapy in a mouse model of renal cell carcinoma (16), PD-L1–based immunotherapy in a mouse model of Braf mutant melanoma was dependent on CD103$^+$ DCs (2). However, in both cases, the role of IL12 was not assessed. Soluble Flt3 ligand and TLR3 adjuvant poly I:C induced activation and expansion of CD103$^+$ DCs *in vivo* and enhanced antitumor immune responses to immune checkpoint blockade by enhancing CTL responses (1, 2).

The DC populations defined by Batf3 and Irf8 expression, though sporadically present on the tumor margins, are functional and superior stimulators for naïve and activated CD8$^+$ T cells (17). Furthermore, the intratumor role of CD103$^+$ DCs was supported by The Cancer Genome Atlas (TCGA) analysis showing that a high *CD103*$^+$/*CD103*$^-$ ratio was associated with better survival (17). Though Batf3-dependent DCs play an important role in T cell–dependent immune responses against primary tumors, their role in antimetastatic innate immune responses remains elusive.

In this study, we used two mouse strains of different genetic backgrounds and a series of experimental and spontaneous metastasis models to determine the intrinsic role of cross-presenting DCs in suppressing metastasis. Here, we show that Batf3 deficiency and Irf8 deficiency in DCs enhanced lung metastasis but did not affect the growth of primary tumors. CD103$^+$ DCs were the major source of IL12 expression in the lungs of mice and were important for controlling metastasis in a NK cell- and IFNγ-dependent manner. In concert, we found that *BATF3* expression was associated with NK cell surface receptors and *IFNγ* expression and both *BATF3* and *IRF8* expression were associated with improved survival of triple-negative breast cancer patients.

Materials and Methods

Mice

C57BL/6 and BALB/c wild-type (WT), and CD45.1 congenic C57BL/6 mice were purchased from the Walter and Eliza Hall Institute for Medical Research or bred in house. C57BL/6 Batf3$^{-/-}$ and BALB/c Batf3$^{-/-}$ mice were originally provided by Ken Murphy (Washington University School of Medicine, St Louis, MO; ref. 7). C57BL/6 IL12p35$^{-/-}$ mice were as previously described (18). C57BL/6 Rag2$^{-/-}$γc$^{-/-}$ mice were obtained from The Jackson Laboratory (ID: 014593). C57BL/6 IRF8$^{fl/fl}$CD11c^{Cre} mice were provided by Dr. Stephen Nutt (Walter and Eliza Hall Institute of Medical Research, Parkville, Australia), and C57BL/6 IL12-YFP reporter mice were provided by Dr. Geoffrey Hill (QIMR Berghofer, Herston, Australia). All mice were bred and maintained at the QIMR Berghofer Medical Research Institute and used between the ages of 8 to 14 weeks. All experiments were approved by the QIMR Berghofer Medical Research Institute Animal Ethics Committee.

Cell culture

Mouse B16F10 melanoma was obtained from the ATCC in 2007 and LWT1 melanoma was derived from SM1WT1 cells at the QIMR Beghofer in 2013. E0771 and 4T1.2 mammary carcinomas were obtained from Dr. Robin Anderson at the Peter MacCallum Cancer Centre (in 2014 and 2004, respectively). All tumor cell lines were maintained in culture for 0 to 14 days and injected as previously described (19). All cell lines were routinely tested negative for *mycoplasma*, but cell line authentication was not routinely performed.

Spontaneous tumor metastasis

For spontaneous metastasis and post-surgery survival experiments, 5×10^4 4T1.2 tumor cells were inoculated into the fourth mammary fat-pad of BALB/c WT and Batf3$^{-/-}$ mice. On day 18, mice were anaesthetized to surgically remove primary tumor and the wound was closed with surgical clips. Some mice additionally received anti-CD4 (GK1.5), anti-CD8β (53.5.8) to deplete T-cell subsets and anti-asialoGM1 to deplete NK cells, and neutralizing anti-IFNγ (H22) as indicated. Survival of the mice was monitored. In some experiments, mice were sacrificed at day 30, and lungs were fixed in Bouin's solution for 24 hours and then washed several times in 70% ethanol. Metastatic tumor nodules were counted under a dissection microscope and lung tissues from 6 to 8 mice were randomly pooled from WT or Batf3$^{-/-}$ mice and embedded in paraffin. Sections were stained with hematoxylin and eosin and slides were scanned through an Aperio slide scanner.

Experimental tumor metastasis

Single-cell suspensions of B16F10 melanoma cells (2×10^5), LWT1 (5×10^5), and 4T1.2 (2×10^4) were injected i.v. into the tail vein of the indicated strains of mice. Some experimental mice additionally received anti-CD4 (GK1.5) and anti-CD8β (53.5.8) to deplete CD4$^+$ and CD8$^+$ T cells, and anti-asialoGM1 to deplete NK cells, and neutralizing anti-IFNγ (H22) as indicated. Lungs were harvested on day 14 and tumor nodules were counted under a dissection microscope.

Flow cytometry analysis

Single-cell suspensions were generated from PBS-perfused lungs from WT and Batf3$^{-/-}$ mice by mincing the lung tissue into small pieces and incubating them with Collagenase type IV (Worthington Chemicals) and DNAse I (Roche) in RPMI for 45 minutes at 37°C. Some samples were incubated with cell-stimulation cocktail (eBioscience) or brefeldin (Biolegend) only for 4 h in complete RPMI medium at 37°C. Samples were washed with PBS and incubated with 2.4G2 (anti-CD16/32) on ice. Cells were stained with antibodies to CD45.2 (104), TCRβ (H57-597), CD8α (53-6.7), CD4 (RM4-5), NK1.1 (PK136), NKp46 (29A1.4), CD49b (Dx5), CD11c (N418), MHC class II (M5/114.15.2), CD103 (2E7), CD11b (M1/70), and CD86 (GL1). The dye Zombie Yellow (Biolegend, BD Biosciences, or eBioscience) was used to distinguish live from dead cells. For intracellular staining, samples were fixed and permeabilized with cytofix/cytoperm kit (BD Biosciences) and stained for anti-IFNγ (XMG1.2) or respective isotype control antibody (Biolegend). To determine absolute number of cells, liquid-counting beads (BD Biosciences) were added directly before samples were run on flow cytometer. All data were collected on an LSR Fortessa 4 (BD Biosciences) flow cytometer and analyzed with FlowJo v10 software (TreeStar, Inc.).

Bone-marrow–derived DC (BMDC) cultures

Bone marrow (BM) cells were prepared from femurs and tibias of WT, Batf3$^{-/-}$ and IL12p35$^{-/-}$ mice. Flt3 ligand was obtained from Celldex Therapeutics and GM-CSF supernatant was derived from a murine erythroleukemia cell line stably transfected to express mouse GM-CSF. GM-CSF and Flt3 ligand-derived BMDCs

Published OnlineFirst October 25, 2017; DOI: 10.1158/2326-6066.CIR-17-0341

were generated as described previously (20). BMDCs were stimulated with 1 μg/mL lipopolysaccharide (LPS) from *E. coli* (Sigma-Aldrich) and BMDCs supernatant was collected after 24 hours.

ELISA

IL12p70 concentration was measured from BMDC supernatants samples with the mouse IL12p70 OptEIA ELISA set (BD Bioscience) as per the manufacturer's instructions. Briefly, maxisorp ELISA plated were coated with anti-IL12p70 in the coating buffer ($Na_2HPO_4 + NaH_2PO_4$) overnight, blocked with 1% BSA for 1 hour and incubated with BMDC supernatants for 2 hours. Samples were subsequently incubated with anti-IL12p70 conjugated to biotin for 2 hours and streptavidin-HRP for 30 minutes before adding TMB substrate. Absorbance was read at 450 nm on a spectrophotometer (BioTek, Millennium Science).

NK cell: tumor cell coculture assays and cytotoxicity

Splenocytes were harvested from WT and Batf3$^{-/-}$ mice and lysed with ACK lysis buffer for 2 minutes. Splenocytes were stained with Mouse NK Cell Isolation Kit II (Miltenyi Biotec) and enriched by a depleting program using LS columns or on AutoMACS-Pro (Miltenyi Biotec) as per the manufacturer's instructions. A total of 1×10^5 NK cells/well were seeded in a round-bottomed 96-well plates with 1:1 supernatant from BMDCs supernatant in the presence or absence of 10 μg/mL of neutralizing anti-IL12 (C17.8, BioXcell). Supernatant was collected after overnight culture and NK cells were stained for surface markers and intracellular IFNγ as described above. To study NK cell–mediated cytotoxicity, purified NK cells were sorted from WT and Batf3$^{-/-}$ mice 24 hours post poly I:C (100 μg per mice) i.p. injection. One million target B16F10 or YAC-1 cells were labeled with 100 μCi/1 of ^{51}Cr and were cocultured for 4 hours with the indicated ratio of primed NK cells.

LPS treatment

Mice were injected intraperitoneally with 200 μg LPS from *E. coli* (Sigma-Aldrich) as described (21). Spleen and lungs were collected 6 hours after the LPS treatment for flow cytometry analysis.

Mixed BM chimeras

BM from femurs and tibias were harvested and red blood cells were lysed with ACK lysis buffer. Recipient WT, Batf3$^{-/-}$, or IL12p35$^{-/-}$ mice were irradiated with two doses of 5.5 Gy of radiation. After 2 to 4 hours of irradiation, the recipient mice were injected intravenously with $2–4 \times 10^6$ BM cells from either a single donor or a 1:1 mixture from two donors as indicated. After 2 months, BM reconstitution was confirmed by flow cytometry analysis on the blood samples using congenic CD45.1/CD45.2 markers of leukocyte populations and chimeric mice were injected i.v. with 2×10^5 B16F10 melanoma cells.

Survival analysis on human samples

Breast cancer RNAseq data generated by TCGA was obtained from the UCSC Cancer Genomics Hub for analysis. Survival plots for different cancer types were plotted using Kaplan Meier (KM) plotter (22). Reads were then trimmed for adapter sequences using Cutadapt (version 1.11) and aligned using STAR (version 2.5.2a) to the GRCH37 assembly using the gene, transcript, and exon features of Ensembl (release 75) gene model (23). Expression was estimated using RSEM (version 1.2.30). Genes with zero read counts across all samples were removed, leaving 1,226 samples with 50,150 genes. Normalization was performed by dividing each sample's gene count by million reads mapped to generate counts per million (CPM), followed by the trimmed mean of M-values (TMM) method from the edgeR package (24).

Statistical analysis

Statistical analysis was achieved using GraphPad Prism Software. Data were compared using a Mann–Whitney *U* test or one-way or two-way ANOVA. Differences in survival were evaluated using a log-rank (Mantel–Cox) test. Data were considered statistically significant where the *P* value was equal to or less than 0.05.

Results

Increased metastasis and poor survival in Batf3-deficient mice

To understand the role of Batf3-dependent DCs in tumor control, we implanted the spontaneously metastasizing 4T1.2 breast cancer cell line in the mammary fat pad of WT and Batf3$^{-/-}$ mice. Unlike primary tumor growth, which was similar in the WT and Batf3$^{-/-}$ mice (Fig. 1A and Supplementary Fig. S1), Batf3$^{-/-}$ mice had increased lung metastasis (Fig. 1B–E) and poorer survival (Fig. 1F), with median survival of 31 days for Batf3$^{-/-}$ mice and 38 days for the WT mice, suggesting that Batf3 was required for metastasis control. A similar pattern of increased lung metastasis was observed in B16F10 melanoma (Fig. 2A), LWT1 Braf-mutant melanoma (Fig. 2B), and 4T1.2 breast carcinoma (Fig. 2C) models of experimental metastases, further suggesting the role of Batf3 in innate immune metastatic control.

To further investigate the role of CD103$^+$ and/or CD8α$^+$ DCs in host control of tumor metastasis, we injected B16F10 melanoma cells in *Irf8*$^{fl/fl}$*CD11c*^{cre} mice previously reported to lack CD8α$^+$CD103$^+$ DCs (25). Consistent with the data obtained from Batf3$^{-/-}$ mice, the lack of *Irf8* expression in CD11c$^+$ DCs (Irf8$^{fl/fl}$CD11c^{cre+}) made no difference to the growth of primary tumors in mice but significantly increased the number of lung metastases compared with their littermate controls (Fig. 2D and Supplementary Fig. S1C), providing further evidence for an important role of CD8α$^+$CD103$^+$ DC in metastasis control.

Increased metastasis in Batf3-deficient mice is NK-cell dependent

Most of the phenotype of Batf3$^{-/-}$ mice has previously been attributed to the poor priming, activation, and function of CD8$^+$ T lymphocytes (7, 26). However, NK cells are the main effectors of antimetastatic activity (27). To investigate the immune effector mechanisms required for Batf3-dependent metastatic control, we depleted CD4$^+$ and CD8$^+$ T lymphocytes or NK cells in the WT and Batf3-deficient mice and examined the effect on the number of lung metastases. The increased number of lung metastases in Batf3$^{-/-}$ mice was independent of CD4$^+$/CD8$^+$ T lymphocytes, as depletion of these cells did not affect the metastatic burden in WT or Batf3$^{-/-}$ mice (Fig. 3A–C). Depletion of CD8$^+$ T cells alone also did not affect survival of 4T1.2 inoculated WT or Batf3$^{-/-}$ mice post-surgical resection of the primary tumor (Fig. 3D). In contrast, depletion of NK cells enhanced the number of lung metastases to an equivalent level in WT mice and Batf3$^{-/-}$ mice in the B16F10, LWT1, and 4T1.2 models of experimental metastases (Fig. 3A–C). Furthermore, depletion of NK cells alone, or together with CD8$^+$ T

Published OnlineFirst October 25, 2017; DOI: 10.1158/2326-6066.CIR-17-0341

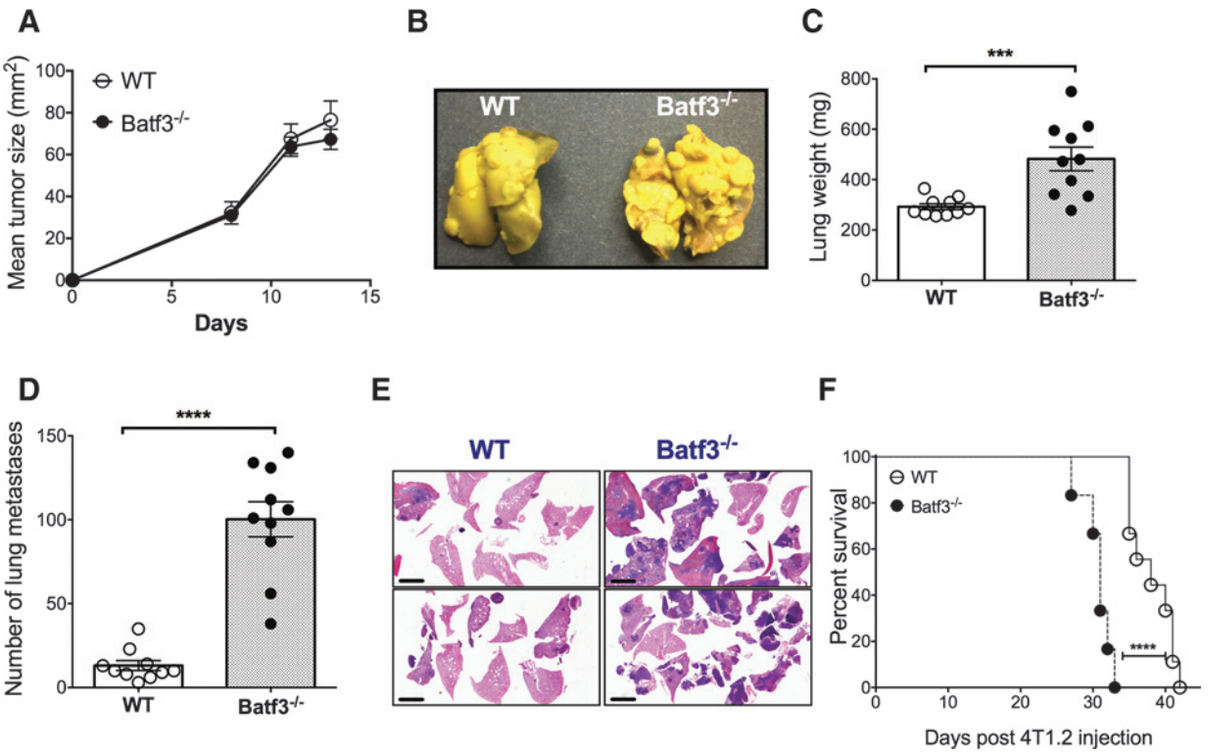

Figure 1.

Increased spontaneous metastasis in Batf3-deficient mice. BALB/c wild-type (WT) and BALB/c Batf3$^{-/-}$ mice were injected in the fourth mammary fat pad with 5×10^4 4T1.2 mammary carcinoma cells and on day-18 primary tumors were resected. **A,** Primary tumor growth, (**B**) representative image of mouse lungs, (**C**) weight of lungs, and (**D**) the number of lung metastases as quantified by counting colonies on the lung surface at day 30 after tumor inoculation. **E,** Lungs were stained with hematoxylin and eosin and representative images of micrometastases are shown. **F,** Survival of mice was monitored. Data represent three independent experiments, and for **C** and **D**, data were pooled from two independent experiments with $n = 5$ mice per experiment. Increased metastasis and poor survival in Batf3$^{-/-}$ mice was statistically significant by the Mann–Whitney test (means ± SEM; ***, $P < 0.001$; ****, $P < 0.0001$) and by log-rank test; ****, $P < 0.0001$. Scale bar, 3 mm.

cell depletion, reduced the overall survival of WT mice but not Batf3$^{-/-}$ mice in the 4T1.2 model of spontaneous cancer metastasis post primary tumor resection (Fig. 3D). In addition, we observed a greater number of NK cells, but not CD4$^+$ or CD8$^+$ T cells, in the lungs of WT mice than Batf3$^{-/-}$ mice in the B16F10 model of experimental lung metastasis (Supplementary Fig. S2), suggesting that NK cells contributed to the innate immune-dependent control of metastasis mediated by Batf3.

NK-cell homeostasis and intrinsic function are normal in Batf3-deficient mice

We hypothesized that intrinsic functional defects in NK cells may contribute to the increased lung metastasis in Batf3$^{-/-}$ mice. However, the frequency of NK cells in the lung, liver, spleen, blood, and BM and their differentiation phenotype with respect to CD11b and CD27 expression were largely similar between naive WT and Batf3$^{-/-}$ mice (Supplementary Fig. S3).

To assess any functional difference in NK cells between WT and Batf3$^{-/-}$ mice during inflammation, we examined NK-cell responses after lipopolysaccharide (LPS) injection *in vivo*. Although LPS activated NK-cell IFNγ production and CD69 expression, the number and activation status of NK cells was similar in the spleens and lungs of WT and Batf3$^{-/-}$ mice following LPS treatment (Supplementary Fig. S4), suggesting that NK cells from Batf3$^{-/-}$ mice have no intrinsic defect and that Batf3-dependent DCs may not be critical for NK-cell responses to LPS.

Next, we examined the antimetastatic function of splenic NK cells from WT and Batf3$^{-/-}$ mice. Adoptive cell transfer (ACT) of splenic NK cells into immunodeficient C57BL/6.Rag2$^{-/-}$γc$^{-/-}$ mice significantly reduces the number of B16F10 lung metastases (28). This activity was independent of Batf3 since the source of NK cells, whether WT or Batf3$^{-/-}$ mice, equivalently reduced the number of lung metastases following transfer (Supplementary Fig. S5A). The peripheral blood of C57BL/6.Rag2$^{-/-}$γc$^{-/-}$ mice showed a similar NK-cell reconstitution following WT or Batf3$^{-/-}$ NK-cell transfer (Supplementary Fig. S5B), suggesting that Batf3 expression in NK cells was not required for reconstitution or intrinsic metastatic activity of NK cells. Furthermore, *in vitro* NK cells from the WT and Batf3$^{-/-}$ mice displayed similar cytotoxic activity towards YAC-1 lymphoma and B16F10 melanoma target cells after stimulation with Poly I:C (Supplementary Fig. S5C). Overall, these results suggest that there is no fundamental functional defect in NK cells from the Batf3$^{-/-}$ mice.

IL12-expressing Batf3-dependent DCs are critical for metastasis suppression

As IL12-producing capability of Batf3-dependent DCs is critical to their immune modulatory function (8, 10, 11, 13, 29–31), we

Published OnlineFirst October 25, 2017; DOI: 10.1158/2326-6066.CIR-17-0341

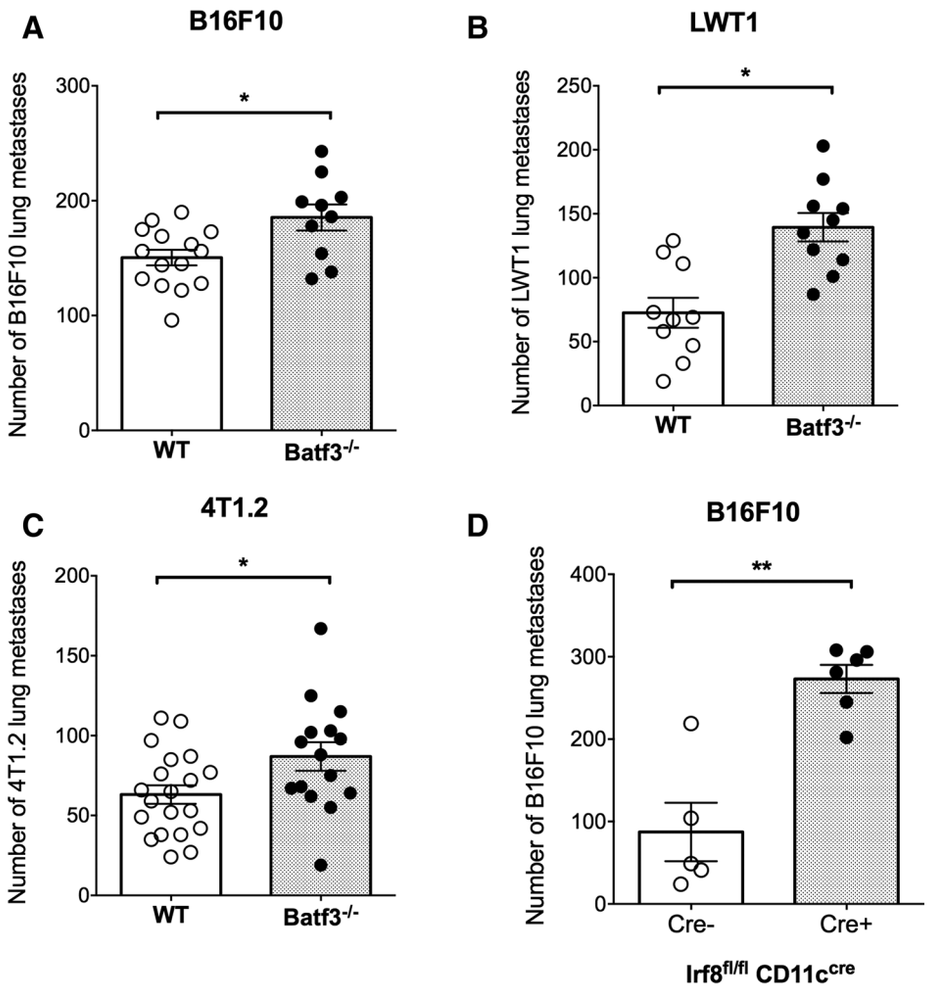

Figure 2.
Increased experimental metastasis in Batf3-deficient mice and mice lacking *Irf8* expression in DCs. C57BL/6 WT and C57BL/6 Batf3$^{-/-}$ mice were injected intravenously with (**A**) B16F10 mouse melanoma (2×10^5) and (**B**) LWT1 melanoma cells (5×10^5). **C,** BALB/c WT and BALB/c Batf3$^{-/-}$ mice were injected intravenously with 4T1.2 mammary carcinoma cells (2×10^4). **D,** B16F10 melanoma cells (2×10^5) were injected intravenously in Irf8$^{fl/fl}$CD11c^{cre+} and Irf8$^{fl/fl}$CD11c^{cre-} mice. Metastatic burden was quantified in the lungs 14 days after tumor inoculation by counting colonies on the lung surface. Means ± SEM of 5 to 15 mice per group are shown. **A–C**, Data pooled from two independent experiments. Mann–Whitney test (*, $P < 0.05$; **, $P < 0.01$).

hypothesized that IL12 from Batf3$^+$ DCs might activate NK-cell antimetastatic activity. As expected, Batf3-deficient mice lacked CD103$^+$ lung DCs (Fig. 4A). Using IL12-YFP reporter mice, we observed a higher proportion of DCs and IL12-expressing CD103$^+$ DCs in the lungs of mice in the B16F10 model of experimental tumor metastasis (Fig. 4A–C). The IL12 expression was detected in the migratory CD103$^+$ DCs; however, resident CD8α$^+$ DCs or CD11b$^+$ myeloid DCs had little or no expression of IL12 (Fig. 4D). Furthermore, the number of CD8α$^+$ DCs in lungs was 10 times lower than CD103$^+$ DCs (Supplementary Fig. S6A). Additionally, IL12-expressing CD103$^+$ DCs had a higher expression of the CD86 activation marker than IL12-negative CD103$^+$ DCs (Fig. 4E). Overall, these results suggest that CD103$^+$ migratory DCs increase in numbers, and they express more IL12 than other DC in the mouse model of experimental B16F10 lung metastasis.

IL12 has antimetastatic function (31, 32) and besides CD103$^+$ DCs, there are other DCs, macrophages, and neutrophils that can potentially contribute to increased IL12 levels. To test whether IL12 from CD103$^+$ Batf3-dependent DCs is the only source of functional protection against metastasis, we generated mixed chimeras using BM from WT, IL12p35$^{-/-}$, and Batf3$^{-/-}$ mice. The mice were bled 2 months after BM transfer to confirm chimerism (Supplementary Fig. S6B). As shown previously, Batf3$^{-/-}$ mice lacked CD8α$^+$/CD103$^+$ DCs, but these DCs developed from the BM of IL12p35$^{-/-}$ mice, despite being unable to produce IL12 (8). In the mixed chimeras reconstituted with IL12p35$^{-/-}$ and Batf3$^{-/-}$ BM, CD8$^+$/CD103$^+$ DCs are the only population that lacks the ability to produce IL12. These mixed chimeric mice displayed very high numbers of B16F10 lung metastases similar to the mice reconstituted with Batf3$^{-/-}$ or IL12p35$^{-/-}$ BM (Fig. 4F). In contrast, mixed chimeric mice reconstituted with WT and Batf3$^{-/-}$ or WT and IL12p35$^{-/-}$ BM displayed half the number of metastases, in concert with only half of the IL12-producing CD8$^+$/CD103$^+$ DCs being available to afford protection from metastasis (Fig. 4F). These results suggest that IL12-producing Batf3-dependent DCs are critical for protection against experimental lung metastasis. Conversely, low-dose recombinant IL12 (rIL12) displayed antimetastatic activity in Batf3$^{-/-}$ mice and WT mice (Fig. 4G), suggesting that even in the absence of the Batf3-dependent DCs, IL12 is capable of providing protection against metastasis.

IL12 from Batf3-dependent DC activates NK cells to release IFNγ

IFNγ from lung resident NK cells is critical for natural resistance to lung metastasis (27) and is essential for the antimetastatic activity of therapeutic rIL12 (30). To assess the role of IFNγ in Batf3-dependent control of lung metastasis, we neutralized IFNγ

Published OnlineFirst October 25, 2017; DOI: 10.1158/2326-6066.CIR-17-0341

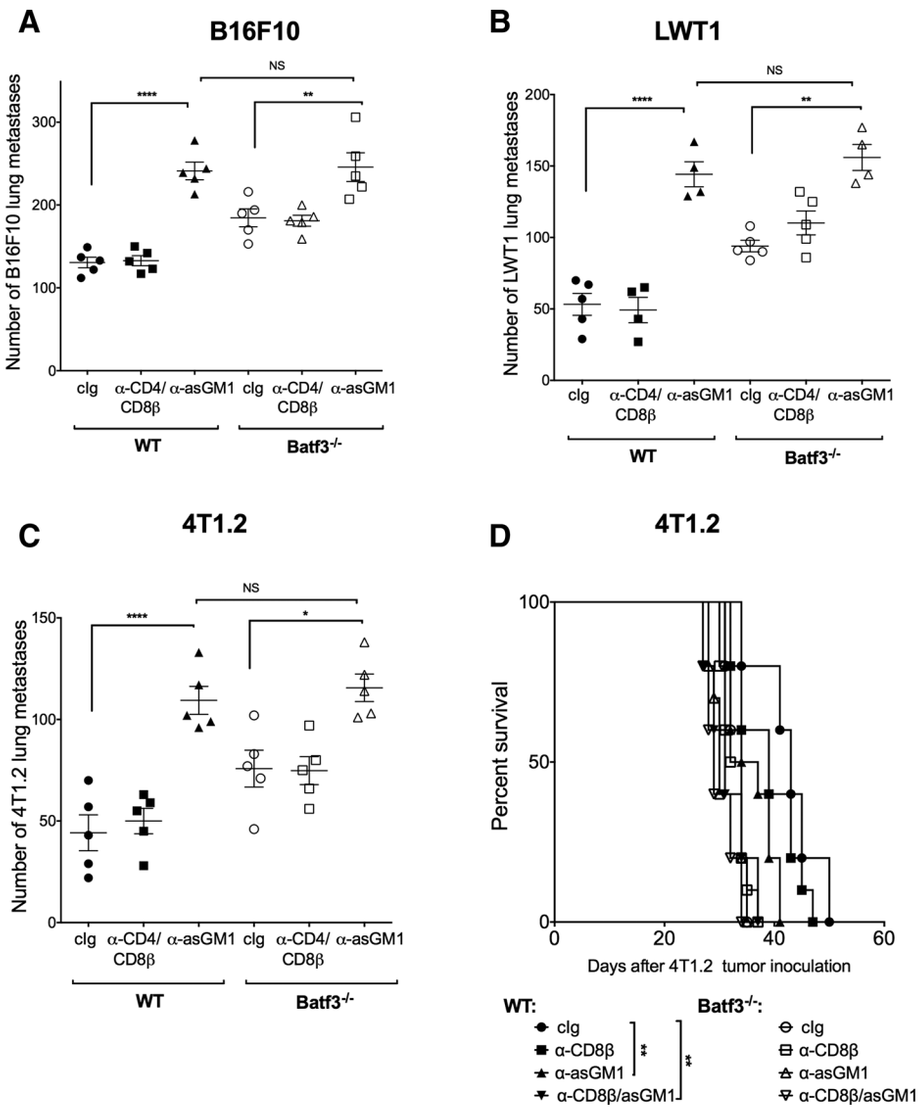

Figure 3.

Increased metastasis in Batf3-deficient mice is NK cell dependent. C57BL/6 WT mice and C57BL/6 Batf3$^{-/-}$ mice (**A**, **B**) and BALB/c WT and BALB/c Batf3$^{-/-}$ mice (**C**) were injected intravenously with (**A**) B16F10 melanoma cells (2×10^5), (**B**) LWT1 melanoma cells (5×10^5) and (**C**) 4T1.2 mammary carcinoma cells (2×10^4) on day 0. Some groups of mice were depleted of NK cells or T cells, by treatment with anti-asGM1 or anti-CD4 and anti-CD8β (100 μg i.p.) on days −1, 0, and 7 as indicated. Metastatic burden was quantified in the lungs after 14 days by counting colonies on the lung surface. Means ± SEM of 5 mice per group are shown. One-way ANOVA test was used (*, $P < 0.05$; **, $P < 0.01$; ****, $P < 0.0001$). **D,** Groups of 5 female BALB/c WT and BALB/c Batf3$^{-/-}$ mice were injected in the mammary fat pad with the mammary carcinoma cell line 4T1.2 (5×10^4). Some groups of mice were depleted of NK cells or T cells, by treatment with anti-asGM1, anti-CD8β or anti-CD8β and anti-asGM1 (100 μg i.p.) on days 17, 18, 25, and 32 as indicated. Survival of the mice was monitored and statistics was performed using log-rank test (**, $P < 0.01$).

in the WT and Batf3$^{-/-}$ mice. Neutralization of IFNγ increased the number of B16F10 experimental lung metastases (Fig. 5A) in WT mice and decreased the survival of WT mice in 4T1.2 model of spontaneous metastasis (Fig. 5B). However, there was no significant change in either the number of lung metastases or the survival of Batf3$^{-/-}$ mice after IFNγ neutralization (Fig. 5A and B), suggesting that IFNγ was required for Batf3-dependent control of lung metastasis. Because increased metastasis in Batf3$^{-/-}$ mice is dependent on both NK cells and IFNγ, we hypothesized that IL12 from CD103$^+$ lung DCs primes NK cells to produce IFNγ that is required for protection against metastasis. To test this hypothesis, we generated CD103$^+$ BM-derived dendritic cells (BMDC) from WT, Batf3$^{-/-}$, and IL12p35$^{-/-}$ mice as described previously (20). BMDCs generated from Batf3$^{-/-}$ produced less IL12 than WT BMDCs after LPS stimulation for 24 hours. As expected, BMDCs from IL12p35$^{-/-}$ mice lacked the ability to produce IL12 (Fig. 5C).

Next, in order to understand whether the IL12 generated from these CD103$^+$ BMDCs could prime NK cells, we cultured WT splenic NK cells with or without supernatant from LPS-stimulated CD103$^+$ BMDCs derived from WT and Batf3$^{-/-}$ mice. The number of IFNγ-expressing NK cells increased when cultured with WT BMDCs compared to the Batf3$^{-/-}$ BMDCs, and the number of IFNγ-expressing NK cells reduced when NK cells were cultured with neutralizing anti-IL12p40 (Fig. 5D). We also observed that NK cells stimulated with WT BMDC supernatant had higher IFNγ expression compared with stimulation with supernatant from Batf3$^{-/-}$ BMDCs, whereas NK cells stimulated with supernatant from IL12p35$^{-/-}$ BMDCs had the lowest IFNγ expression (Supplementary Fig. S7). These results suggested that IL12 from CD103$^+$ BMDCs activated NK cells to produce IFNγ. To test IFNγ from NK cells *in vivo*, we collected lungs from WT and Batf3$^{-/-}$ mice 3 days after B16F10 tumor injection. Control and tumor-bearing lungs in WT mice had more IFNγ$^+$ NK cells than did lungs of Batf3$^{-/-}$ mice (Fig. 5E). Also, after stimulation with cell-stimulation cocktail, IFNγ$^+$ NK cells were significantly more numerous in the tumor-bearing lungs of WT mice than in the lungs of Batf3$^{-/-}$ mice (Fig. 5F). Overall, these results suggest that IL12 from Batf3-dependent DCs may activate NK cells to produce IFNγ.

Published OnlineFirst October 25, 2017; DOI: 10.1158/2326-6066.CIR-17-0341

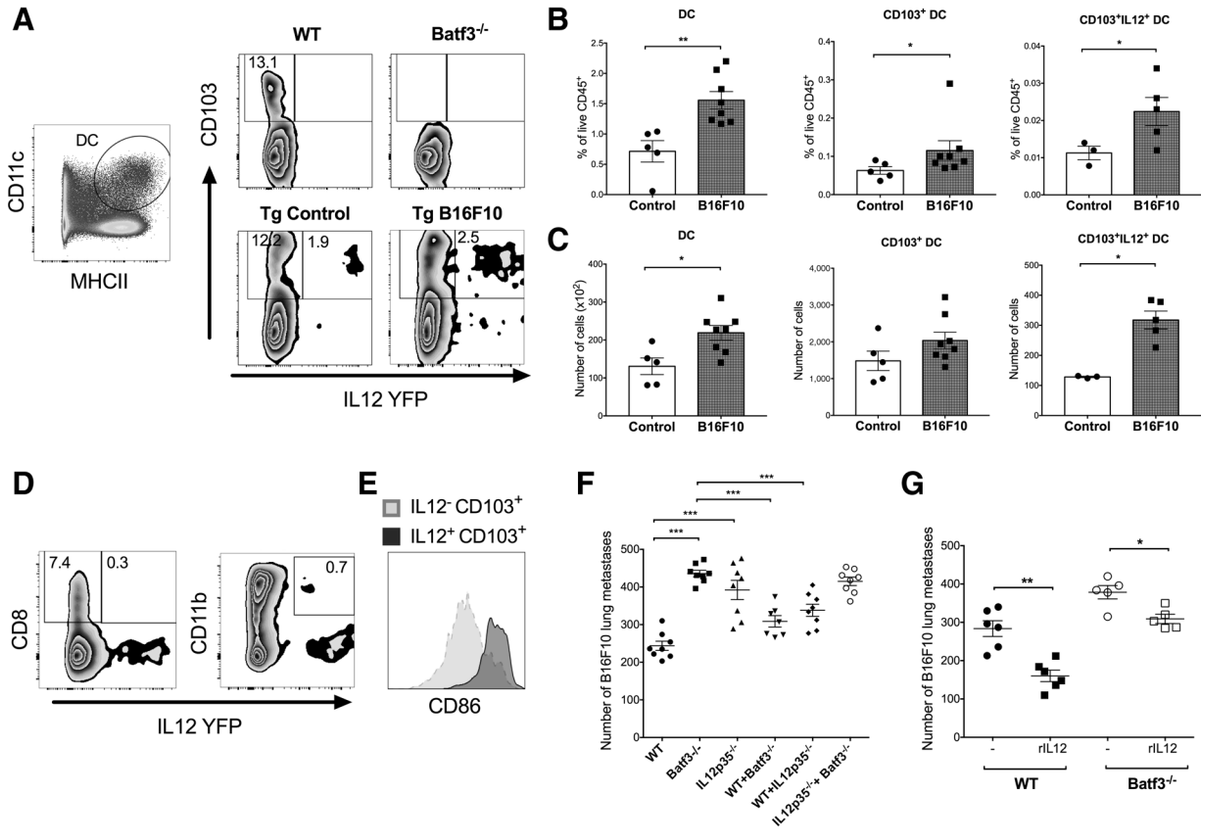

Figure 4.

IL12-expressing CD103$^+$ Batf3-dependent DCs are critical for suppressing experimental lung metastasis. Lungs from C57BL/6 WT, C57BL/6 Batf3$^{-/-}$, and C57BL/6 IL12-YFP reporter mice were harvested for flow cytometry 1 day after intravenous B16F10 (2×10^5 cells) melanoma injection. **A,** FACS plot showing IL12-YFP and CD103 expression in CD11c$^+$ MHCII$^+$ DCs population pre-gated on live CD45$^+$ population in WT mice, Batf3$^{-/-}$ mice and IL12-YFP transgenic mice injected with PBS (Tg control) or B16F10 (Tg B16F10). **B,** Percentage and (**C**) absolute number of total DCs, CD103$^+$ DCs, and IL12 expressing CD103$^+$ DCs in the lungs of IL12-YFP reporter mice injected with PBS control or B16F10 melanoma cell line. Data were pooled from two independent experiments. **D,** FACS plot showing IL12 expression in CD8α^+ and CD11b$^+$ DCs pre-gated on live DCs. **E,** A representative histograms showing CD86 expression in IL12$^-$ and IL12$^+$ CD103$^+$ DCs population. B16F10 melanoma cells (2×10^5) were injected intravenously into (**F**) mice reconstituted with mixed BM (1:1) two months after reconstitution and (**G**) WT and Batf3$^{-/-}$ mice injected i.p. with 10 μg recombinant IL12 on days 0, 1, 3, and 5. Metastatic burden was quantified in the lungs after 14 days by counting colonies on the lung surface. Means ± SEM of 5–8 mice per group are shown. Data from (**G**) are representative of two independent experiments. Mann–Whitney (**B**, **C**) or one-way ANOVA (**F**, **G**) test was used (*, $P < 0.05$; **, $P < 0.01$; ***, $P < 0.001$).

BATF3 and *IRF8* expression, NK-cell markers, and breast cancer patient survival

Immunoscore using a high *CD103*$^+$/*CD103*$^-$ gene expression ratio had a profound effect on increased survival in breast cancer, head and neck squamous cell carcinoma and lung adenocarcinoma (17). Given the fact that Batf3- and Irf8 deficiency promoted mouse lung tumor metastasis, we wished to test whether intratumor expression of Batf3 and Irf8 in humans might predict patient survival (22).

Using TCGA data sets, we observed that a higher expression of *BATF3* and *IRF8* was associated with a minor, but statistically significant, improvement in relapse-free survival of breast cancer patients (Fig. 6A). Additionally, the high expression of *IL12*, NK cell–associated genes (*CD56*, *NKP46*, and *NKG2D*) and *IFNG* (*IFNγ*) was also associated with improved survival (Fig. 6A). The cDC-specific gene, *Zbtb46*, is efficiently induced by Irf8 (33), and CCR7 is reportedly expressed by all CD103$^+$ DCs (20). We found high expression of *CCR7* and *ZBTB46* associated with improved patient outcome (Fig. 6A). The correlations between *BATF3*, *CD103* or *IRF8* expression and relapse-free survival were even more significant in metastatic triple-negative breast cancer (TNBC) patients amongst all breast cancer patients (Fig. 6B). High expression of *BATF3*, *CD103*, and *IRF8* correlated (P range = 0.0035–0.046) with relapse-free survival of poorly differentiated high-grade (grade 3) breast cancers, but not for lower grade breast cancers (Supplementary Fig. S8), suggesting that Batf3-dependent DCs are important in controlling highly aggressive metastatic cancers. Additionally, high expression of *IRF8* significantly correlated with progression-free survival in gastric cancers (Fig. 6C) and lung cancers (Fig. 6D).

Next, to determine if a Batf3-dependent DCs–NK-cell axis was important for host control of metastasis, we used TCGA data to quantify correlations among relative gene expression for breast cancers. As expected, *BATF3* and *IRF8* expression was highly correlated with DC markers *CD103*, *CCR7*, and *CD86* in both normal breast tissues and breast cancers (Supplementary Fig. S9).

Published OnlineFirst October 25, 2017; DOI: 10.1158/2326-6066.CIR-17-0341

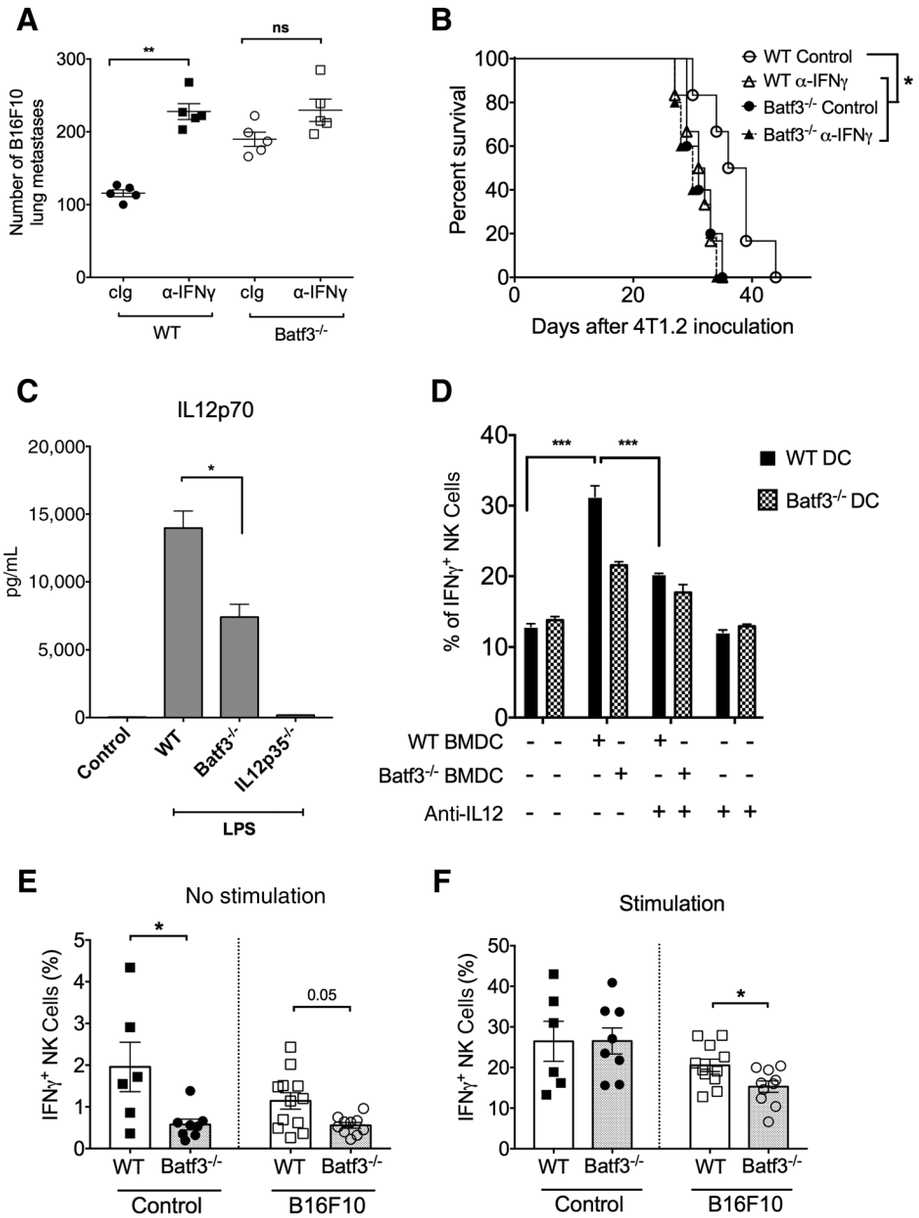

Figure 5.

IL12 from CD103$^+$ Batf3-dependent DCs stimulates NK-cell IFNγ production. **A,** B16F10 melanoma cells (2×10^5) were injected intravenously into WT and Batf3$^{-/-}$ mice and neutralizing anti-IFNγ (250 μg) was injected i.p. on days 0, 1, and 7. Metastatic burden was quantified in the lungs after 14 days by counting colonies on the lung surface. $n = 5$ mice/group. **B,** 4T1.2 tumor cells (5×10^4) were injected into the fourth mammary fat pad of WT and Batf3$^{-/-}$ mice and 250 μg of neutralizing anti-IFNγ was injected i.p. on days 11, 13, and 20. Primary tumors were resected on day 14, and survival of mice was monitored. **C,** IL12 production from WT, Batf3$^{-/-}$, and IL12p35$^{-/-}$ BMDC cultures stimulated or not (WT control) for 24 hours with 1 μg/mL LPS. **D,** MACS-sorted splenic NK cells from WT mice were cultured with LPS-stimulated WT BMDC, Batf3$^{-/-}$ BMDC, or IL12p35$^{-/-}$ BMDC medium (1:1) overnight in the presence or absence of 10 μg/mL neutralizing anti-IL12p40. Percentages of IFNγ$^+$ NK cells are shown as determined by flow cytometry. **E** and **F,** B16F10 melanoma cells (2×10^5) were injected i.v. into WT and Batf3$^{-/-}$ mice and lungs were collected at day 3. Percentages of IFNγ$^+$ NK cells are shown from control and tumor-bearing lungs of WT and Batf3$^{-/-}$ mice incubated for 4 hours with brefeldin (**E**) or stimulated with cell-stimulation cocktail (**F**). Data were pooled from two independent experiments with $n = 3$–6 mice/experiment. Log-rank test was used for **B**, one-way ANOVA test used for statistical comparison between groups in **A**, **C**, and **D**, and Mann–Whitney test was used in **E** and **F** (*, $P < 0.05$; **, $P < 0.01$; ***, $P < 0.001$; ns, not significant).

BATF3 and *IRF8* expression was significantly positively correlated with DC effector *IL12A* only in breast cancers (Supplementary Fig. S10) and was also more positively correlated with NK-cell markers such as *KLRK1*, *NCAM1* (encoding NKG2D), and the effector cytokine *IFNG* in breast cancer tissues than in normal control tissues (Supplementary Fig. S10). *CD103* expression also showed positive correlations with *KLRK1* and *IFNG* in breast cancers compared with the normal tissue. This supports our hypothesis and suggests that IL12-expressing BATF3-dependent DCs and IFNγ from NK cells may form an important functional axis for intrinsic tumor control in breast cancers.

Discussion

Metastasis is the leading cause of cancer-related deaths worldwide. Better understanding of host mechanisms that can suppress metastasis is required to successfully develop therapies targeting cancer metastasis. NK cells are innate lymphocytes that play a central role in host rejection of tumors and virus-infected cells. We have previously shown that perforin and IFNγ from NK cells is critical for providing natural resistance to tumor metastasis to lung (27, 34). Dendritic cells, which are required for priming and activation of CTL activity, are also responsible for increases in NK cell–cytolytic activity and IFNγ production (35). DC- and NK-cell cross-talk may be dependent on receptor–ligand contacts (35) or IL12 secretion from DCs that primes NK cells for IFNγ production (29–31). In this study, we show that CD103$^+$ Batf3-dependent cross-presenting DCs are potent producers of IL12 in lungs and may partially activate host resistance to metastasis in the lung by mechanisms dependent on NK cells and IFNγ.

Batf3 is critical for protection against lung metastasis. Despite similar primary tumor growth, Batf3-deficient mice had enhanced

Published OnlineFirst October 25, 2017; DOI: 10.1158/2326-6066.CIR-17-0341

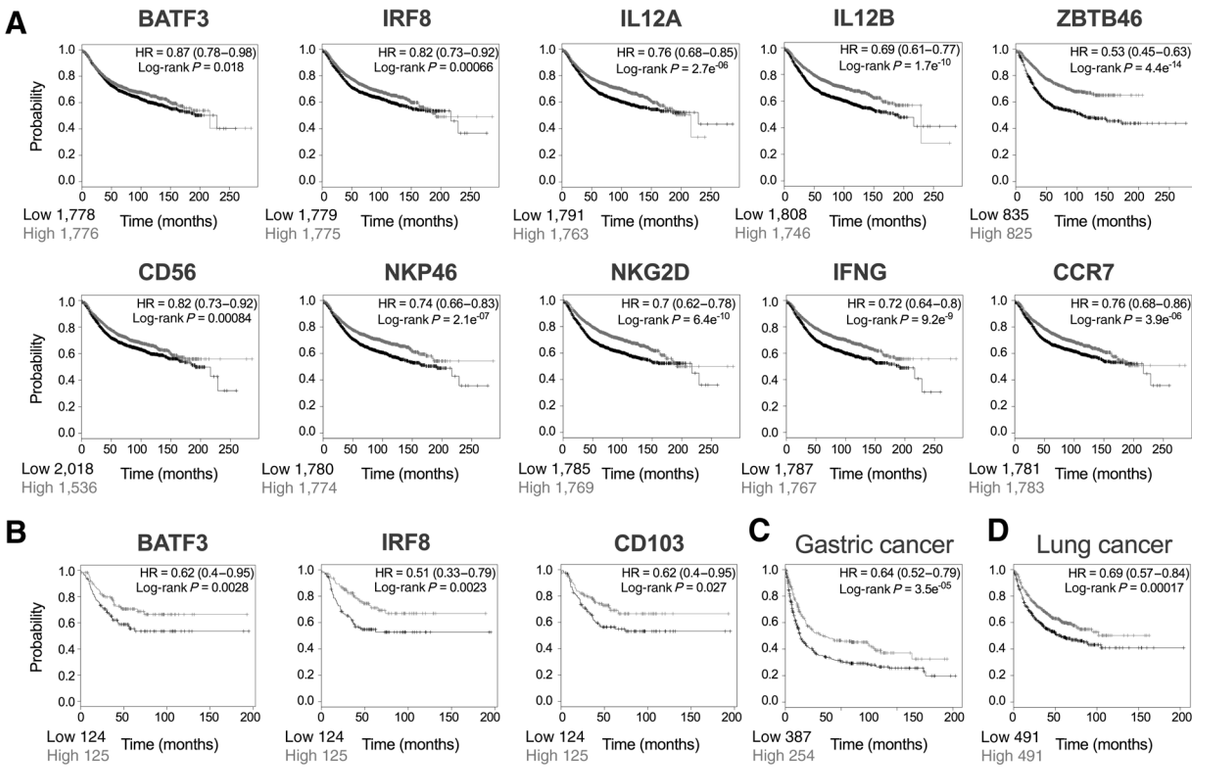

Figure 6.

BATF3 and *IRF8* expression is associated with increased survival of cancer patients. Kaplan–Meier (KM) survival curves showing association of (**A**) *BATF3, IRF8, IL12A, IL12B, ZBTB46, CD56, NKP46, NKG2D, IFNG,* and *CCR7* expression with relapse-free survival in all breast cancers, (**B**) *BATF3,IRF8,* and *CD103* expression with relapse-free survival in TNBCs, and *IRF8* expression with progression-free survival in gastric cancers (**C**) and lung cancers (**D**) obtained from KM plotter. Log-rank *P* value with hazard ratio (HR) is shown for each km plot. High expression is shown in gray and low in black.

experimental and spontaneous lung metastasis compared with the WT mice. The increased lung metastasis phenotype in mice that specifically lacked *Irf8* expression in CD11c$^+$ DC subsets suggested that cross-presenting DCs, mainly CD103$^+$ DCs, are partially required for NK-cell resistance to metastasis, because Batf3-deficient mice may still develop CD8α^+ DCs, but not CD103$^+$ DCs, under certain conditions (36–39). In support, we found an increased number of IL12-expressing CD103$^+$ DCs, but not tissue-resident CD8α^+ DCs, in the lungs of mice injected with B16F10 melanoma cells. The role of IL12 from Batf3-dependent DCs in suppressing metastasis was confirmed by mixed BM chimeras where the mixed BM from IL12$^{-/-}$ and Batf3$^{-/-}$ mice, but not WT and IL12$^{-/-}$ or WT and Batf3$^{-/-}$ mice, failed to provide protection against B16F10 lung metastasis. Further, IL12 administration in Batf3-deficient mice partially restored host protection against lung metastasis. Our results in a tumor metastasis model were in concert with a previously published report where mixed BM chimeric mice that specifically lacked IL12 from Batf3$^+$ DCs were as susceptible to *Toxoplasma gondii* infection as Batf3$^{-/-}$ mice (8).

The majority of Batf3-dependent immune responses against tumors and infection require activation and cytotoxic activity of CD8$^+$ T lymphocytes (1, 2, 7, 8, 13, 14, 16, 17, 26). However, both CD4$^+$ and CD8$^+$ T lymphocytes are dispensable for metastatic control by Batf3-depedent DCs. Instead, Batf3-dependent control of metastasis required NK cells and IFNγ. Dendritic cells can activate NK cells by forming a stimulatory synapse that can polarize IL12 secretion specifically into NK cells (29) or DC-derived exosomes can activate NK cells via a TNF pathway (40). CD103$^+$ Batf3-dependent lung DCs were shown to acquire and cross-present apoptotic cell-associated antigen to CD8$^+$ T cells (5). It is possible that antigens from metastatic tumor cells in the lungs are taken up by tissue-resident CD103$^+$ DCs that then release IL12 to activate lung-resident NK cells for IFNγ production and protection against metastasis. Taken together, our data suggest a pathway comprising Batf3-dependent DCs that produce IL12, which then stimulates NK cells to produce IFNγ and partially control tumor cell metastasis. The partial effect of Batf3 and IL12 was consistent with a demonstrated role of myeloid-derived IFNs α,β, and λ, as well as NK-cell perforin, in experimental metastasis control (34, 41).

CD103$^+$ DCs are sparse and proximal to the tumor margins but can interact with intratumor T cells for effective adoptive CTL therapy (17). In humans, the transcript signature ratio of CD103$^+$ to CD103$^-$ tumor-associated macrophages provided a strong prognostic signal across multiple tumor types in TCGA data. This ratio was more informative than other commonly used immune-based prognostic gene expression markers (17). In concert, we observed higher expression of *BATF3, IRF8*, NK-cell markers and *IFNγ* associated with improved relapse-free survival in breast cancer patients. Furthermore, we found a significant correlation between *BATF3* expression and *IL12, IFNγ* and NK cell-associated

Published OnlineFirst October 25, 2017; DOI: 10.1158/2326-6066.CIR-17-0341

markers in tumors from TCGA datasets suggesting that Batf3-dependent DCs in association with NK cells and IFNγ may form an important functional axis for metastasis control.

Immune checkpoint blockade by anti–PD-L1 and the combination of anti-PD-1 and agonistic anti-CD137 requires Batf3-dependent DCs (1, 2), suggesting that impairment of Batf3-dependent DC function may be one mechanism that causes some patients to respond poorly to immune checkpoint blockade. Our studies demonstrate that $CD103^+$ Batf3-dependent DCs provide natural resistance to metastasis and encourage the use of reagents, such as TLR3-adjuvant poly I:C and Flt3 ligand, that activate these DCs (42, 43) and may enhance the antimetastatic efficacy of current cancer therapies.

Disclosure of Potential Conflicts of Interest

M.J. Smyth reports receiving commercial research grants from Bristol-Myers Squibb, Aduro Biotech, Tizona Therapeutics, and Corvus Pharmaceuticals; is a consultant/advisory board member for Tizona Therapeutics; and has provided expert testimony for Corvus Pharmaceuticals. No conflicts of interest were disclosed by the other authors.

Authors' Contributions

Conception and design: D. Mittal, M.J. Smyth
Development of methodology: D. Mittal, D. Vijayan, A.R. Aguilera
Acquisition of data (provided animals, acquired and managed patients, provided facilities, etc.): D. Mittal, E.M. Putz, A.R. Aguilera, K.A. Markey, S.L. Nutt, M.J. Smyth
Analysis and interpretation of data (e.g., statistical analysis, biostatistics, computational analysis): D. Mittal, A.R. Aguilera, J. Straube, S. Kazakoff, N. Waddell, M.J. Smyth
Writing, review, and/or revision of the manuscript: D. Mittal, K.A. Markey, G.R. Hill, M.J. Smyth
Administrative, technical, or material support (i.e., reporting or organizing data, constructing databases): K. Takeda
Study supervision: D. Mittal, M.J. Smyth

Acknowledgments

M.J. Smyth was supported by a National Health and Medical Research Council of Australia (NHMRC) Senior Principal Research Fellowship (1078671) and Program Grant (1013667), and S.L. Nutt was supported by an NHMRC Principal Research Fellowship (1058238) and Program Grant (1054925). E.M. Putz was supported by an Erwin Schroedinger Fellowship of the Austrian Science Fund (J-3635). K.A. Markey is a Queensland Health Junior Clinical Research Fellow. We thank Kate Elder and Liam Town for their technical support with breeding and genotyping of mice. We also thank Fernando Souza-FonsecaGuimaraes and Stuart Olver for their technical help with the cytotoxicity experiments.

The costs of publication of this article were defrayed in part by the payment of page charges. This article must therefore be hereby marked *advertisement* in accordance with 18 U.S.C. Section 1734 solely to indicate this fact.

Received June 29, 2017; revised September 19, 2017; accepted October 17, 2017; published OnlineFirst October 25, 2017.

References

1. Sanchez-Paulete AR, Cueto FJ, Martinez-Lopez M, Labiano S, Morales-Kastresana A, Rodriguez-Ruiz ME, et al. Cancer immunotherapy with immunomodulatory anti-CD137 and anti-PD-1 monoclonal antibodies requires BATF3-dependent dendritic cells. Cancer Discov 2016;6:71–9.
2. Salmon H, Idoyaga J, Rahman A, Leboeuf M, Remark R, Jordan S, et al. Expansion and activation of CD103(+) dendritic cell progenitors at the tumor site enhances tumor responses to therapeutic PD-L1 and BRAF inhibition. Immunity 2016;44:924–38.
3. Corrales L, Matson V, Flood B, Spranger S, Gajewski TF. Innate immune signaling and regulation in cancer immunotherapy. Cell Res 2017;27:96–108.
4. Gardner A, Ruffell B. Dendritic cells and cancer immunity. Trends Immunol 2016;37:855–65.
5. Desch AN, Randolph GJ, Murphy K, Gautier EL, Kedl RM, Lahoud MH, et al. CD103+ pulmonary dendritic cells preferentially acquire and present apoptotic cell-associated antigen. J Exp Med 2011;208:1789–97.
6. Joffre OP, Segura E, Savina A, Amigorena S. Cross-presentation by dendritic cells. Nat Rev Immunol 2012;12:557–69.
7. Hildner K, Edelson BT, Purtha WE, Diamond M, Matsushita H, Kohyama M, et al. Batf3 deficiency reveals a critical role for CD8alpha+ dendritic cells in cytotoxic T cell immunity. Science 2008;322:1097–100.
8. Mashayekhi M, Sandau MM, Dunay IR, Frickel EM, Khan A, Goldszmid RS, et al. CD8alpha(+) dendritic cells are the critical source of interleukin-12 that controls acute infection by Toxoplasma gondii tachyzoites. Immunity 2011;35:249–59.
9. Ashok D, Schuster S, Ronet C, Rosa M, Mack V, Lavanchy C, et al. Cross-presenting dendritic cells are required for control of Leishmania major infection. Eur J Immunol 2014;44:1422–32.
10. Torres D, Kohler A, Delbauve S, Caminschi I, Lahoud MH, Shortman K, et al. IL-12p40/IL-10 producing preCD8alpha/Clec9A$^+$ dendritic cells are induced in neonates upon Listeria monocytogenes infection. PLoS Pathog 2016;12:e1005561.
11. Everts B, Tussiwand R, Dreesen L, Fairfax KC, Huang SC, Smith AM, et al. Migratory $CD103^+$ dendritic cells suppress helminth-driven type 2 immunity through constitutive expression of IL-12. J Exp Med 2016;213:35–51.
12. Break TJ, Hoffman KW, Swamydas M, Lee CC, Lim JK, Lionakis MS. Batf3-dependent CD103(+) dendritic cell accumulation is dispensable for mucosal and systemic antifungal host defense. Virulence 2016;7:826–35.
13. Martinez-Lopez M, Iborra S, Conde-Garrosa R, Sancho D. Batf3-dependent $CD103^+$ dendritic cells are major producers of IL-12 that drive local Th1 immunity against Leishmania major infection in mice. Eur J Immunol 2015;45:119–29.
14. Waithman J, Zanker D, Xiao K, Oveissi S, Wylie B, Ng R, et al. Resident CD8(+) and migratory CD103(+) dendritic cells control CD8 T cell immunity during acute influenza infection. PLoS One 2013;8:e66136.
15. Zitvogel L, Kroemer G. CD103+ dendritic cells producing interleukin-12 in anticancer immunosurveillance. Cancer Cell 2014;26:591–3.
16. James BR, Brincks EL, Kucaba TA, Boon L, Griffith TS. Effective TRAIL-based immunotherapy requires both plasmacytoid and CD8alpha dendritic cells. Cancer Immunol Immunother 2014;63:685–97.
17. Broz ML, Binnewies M, Boldajipour B, Nelson AE, Pollack JL, Erle DJ, et al. Dissecting the tumor myeloid compartment reveals rare activating antigen-presenting cells critical for T cell immunity. Cancer Cell 2014;26:638–52.
18. Teng MW, Andrews DM, McLaughlin N, von Scheidt B, Ngiow SF, Moller A, et al. IL-23 suppresses innate immune response independently of IL-17A during carcinogenesis and metastasis. Proc Natl Acad Sci USA 2010;107:8328–33.
19. Mittal D, Sinha D, Barkauskas D, Young A, Kalimutho M, Stannard K, et al. Adenosine 2B receptor expression on cancer cells promotes metastasis. Cancer Res 2016;76:4372–82.
20. Mayer CT, Ghorbani P, Nandan A, Dudek M, Arnold-Schrauf C, Hesse C, et al. Selective and efficient generation of functional Batf3-dependent $CD103^+$ dendritic cells from mouse bone marrow. Blood 2014;124:3081–91.
21. Chan CJ, Martinet L, Gilfillan S, Souza-Fonseca-Guimaraes F, Chow MT, Town L, et al. The receptors CD96 and CD226 oppose each other in the regulation of natural killer cell functions. Nat Immunol 2014;15:431–8.
22. Szasz AM, Lanczky A, Nagy A, Forster S, Hark K, Green JE, et al. Cross-validation of survival associated biomarkers in gastric cancer using transcriptomic data of 1,065 patients. Oncotarget 2016;7:49322–33.

23. Dobin A, Davis CA, Schlesinger F, Drenkow J, Zaleski C, Jha S, et al. STAR: ultrafast universal RNA-seq aligner. Bioinformatics 2013;29:15–21.
24. Robinson MD, McCarthy DJ, Smyth GK. edgeR: a Bioconductor package for differential expression analysis of digital gene expression data. Bioinformatics 2010;26:139–40.
25. Chopin M, Seillet C, Chevrier S, Wu L, Wang H, Morse HC 3rd, et al. Langerhans cells are generated by two distinct PU.1-dependent transcriptional networks. J Exp Med 2013;210:2967–80.
26. Fuertes MB, Kacha AK, Kline J, Woo SR, Kranz DM, Murphy KM, et al. Host type I IFN signals are required for antitumor CD8+ T cell responses through CD8{alpha}+ dendritic cells. J Exp Med 2011;208:2005–16.
27. Takeda K, Nakayama M, Sakaki M, Hayakawa Y, Imawari M, Ogasawara K, et al. IFN-gamma production by lung NK cells is critical for the natural resistance to pulmonary metastasis of B16 melanoma in mice. J Leukoc Biol 2011;90:777–85.
28. Martinet L, Ferrari De Andrade L, Guillerey C, Lee JS, Liu J, Souza-Fonseca-Guimaraes F, et al. DNAM-1 expression marks an alternative program of NK cell maturation. Cell Rep 2015;11:85–97.
29. Borg C, Jalil A, Laderach D, Maruyama K, Wakasugi H, Charrier S, et al. NK cell activation by dendritic cells (DCs) requires the formation of a synapse leading to IL-12 polarization in DCs. Blood 2004;104:3267–75.
30. Hafner M, Falk W, Echtenacher B, Mannel DN. Interleukin-12 activates NK cells for IFN-gamma-dependent and NKT cells for IFN-gamma-independent antimetastatic activity. Eur Cytokine Netw 1999;10:541–8.
31. Takeda K, Hayakawa Y, Atsuta M, Hong S, Van Kaer L, Kobayashi K, et al. Relative contribution of NK and NKT cells to the anti-metastatic activities of IL-12. Int Immunol 2000;12:909–14.
32. Lasek W, Zagozdzon R, Jakobisiak M. Interleukin 12: still a promising candidate for tumor immunotherapy? Cancer Immunol Immunother 2014;63:419–35.
33. Jaiswal H, Kaushik M, Sougrat R, Gupta M, Dey A, Verma R, et al. Batf3 and Id2 have a synergistic effect on Irf8-directed classical CD8alpha+ dendritic cell development. J Immunol 2013;191:5993–6001.
34. Street SE, Cretney E, Smyth MJ. Perforin and interferon-gamma activities independently control tumor initiation, growth, and metastasis. Blood 2001;97:192–7.
35. Fernandez NC, Lozier A, Flament C, Ricciardi-Castagnoli P, Bellet D, Suter M, et al. Dendritic cells directly trigger NK cell functions: cross-talk relevant in innate anti-tumor immune responses in vivo. Nat Med 1999;5:405–11.
36. Mott KR, Maazi H, Allen SJ, Zandian M, Matundan H, Ghiasi YN, et al. Batf3 deficiency is not critical for the generation of CD8alpha(+) dendritic cells. Immunobiology 2015;220:518–24.
37. Murphy TL, Tussiwand R, Murphy KM. Specificity through cooperation: BATF-IRF interactions control immune-regulatory networks. Nat Rev Immunol 2013;13:499–509.
38. Seillet C, Jackson JT, Markey KA, Brady HJ, Hill GR, Macdonald KP, et al. CD8alpha+ DCs can be induced in the absence of transcription factors Id2, Nfil3, and Batf3. Blood 2013;121:1574–83.
39. Tussiwand R, Lee WL, Murphy TL, Mashayekhi M, Kc W, Albring JC, et al. Compensatory dendritic cell development mediated by BATF-IRF interactions. Nature 2012;490:502–7.
40. Munich S, Sobo-Vujanovic A, Buchser WJ, Beer-Stolz D, Vujanovic NL. Dendritic cell exosomes directly kill tumor cells and activate natural killer cells via TNF superfamily ligands. Oncoimmunology 2012;1:1074–83.
41. Souza-Fonseca-Guimaraes F, Young A, Mittal D, Martinet L, Bruedigam C, Takeda K, et al. NK cells require IL-28R for optimal in vivo activity. Proc Natl Acad Sci USA 2015;112:E2376–84.
42. Guillerey C, Chow MT, Miles K, Olver S, Sceneay J, Takeda K, et al. Toll-like receptor 3 regulates NK cell responses to cytokines and controls experimental metastasis. Oncoimmunology 2015;4:e1027468.
43. Peron JM, Esche C, Subbotin VM, Maliszewski C, Lotze MT, Shurin MR. FLT3-ligand administration inhibits liver metastases: role of NK cells. J Immunol 1998;161:6164–70.

Published OnlineFirst October 25, 2017; DOI: 10.1158/2326-6066.CIR-17-0341

Cancer Immunology Research

Interleukin-12 from CD103$^+$ Batf3-Dependent Dendritic Cells Required for NK-Cell Suppression of Metastasis

Deepak Mittal, Dipti Vijayan, Eva M. Putz, et al.

Cancer Immunol Res 2017;5:1098-1108. Published OnlineFirst October 25, 2017.